eprints@whiterose.ac.uk
https://eprints.whiterose.ac.uk/

Scalable and sustainable manufacturing of ultrathin metal-organic framework nanosheets (MONs) for solar cell applications

Authors

David J. Ashworth[a], Justin Driver[a,b], Kezia Sasitharan[a], Ram R. R. Prasad[a], Joshua Nicks[a], Benedict J. Smith[a], Siddharth V. Patwardhan[b] and Jonathan A. Foster[a,*]

Addresses

[a]   Department of Chemistry, The University of Sheffield, Brook Hill, Sheffield, S3 7HF, UK.
[b]   Department of Chemical and Biological Engineering, The University of Sheffield, Mappin Street, Sheffield, S1 3JD, UK.

*Corresponding author e-mail address: jona.foster@sheffield.ac.uk

Electronic Supplementary Information

Contents

1. H₆TCPP synthesis

Fig. S1. ¹H NMR spectrum of H$_6$TCPP in d_6-DMSO. H$_d$ are not integrated due to broad signal, and part-exchange with D atoms in solution leading to under-representation. Peaks marked (*) correspond to small amounts of propionic acid starting reagent; 2.22 (q, 2H, CH$_2$), 0.99 (t, 3H, CH$_3$)
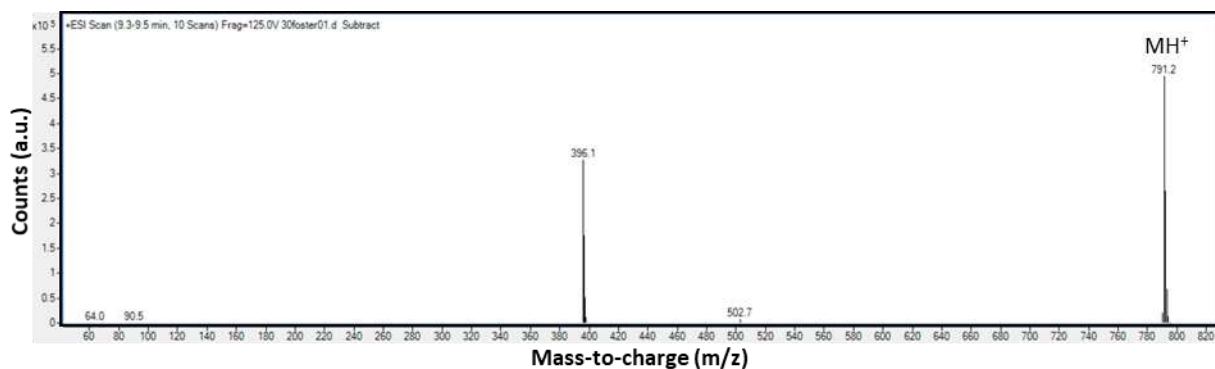
Fig. S2. MS spectrum of H$_6$TCPP. H$_6$TCPP (C$_{48}$H$_{30}$N$_4$O$_8$) m/z = 790.2. MH⁺ m/z = 791.2.
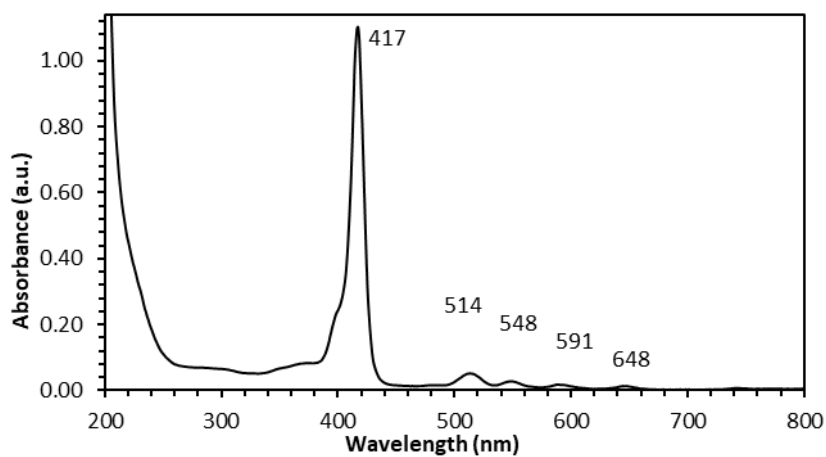
Fig. S3. UV-Vis spectrum of H$_6$TCPP in EtOH.
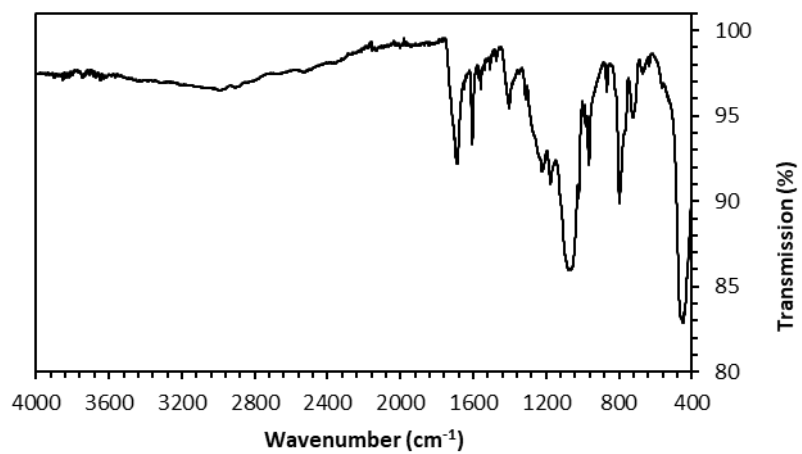
Fig. S4. ATR-FTIR spectrum of H_6TCPP.

2. Zn$_2$(ZnTCPP) MOF syntheses using batch conditions
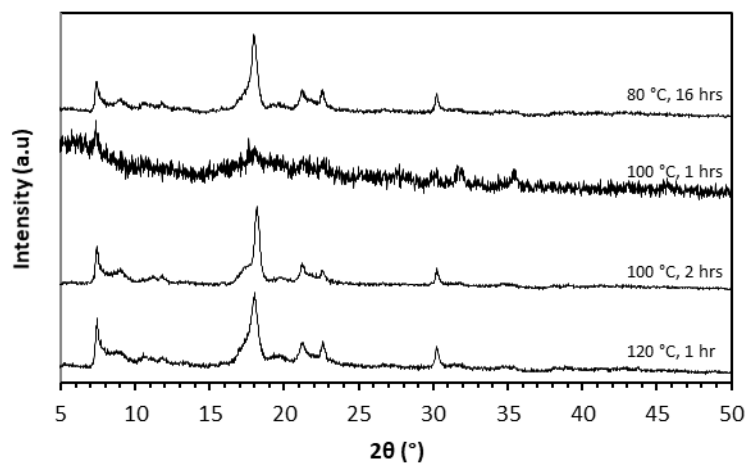
Fig. S5. PXRD patterns of solids produced from batch reaction (0.0625 wt%) at various time-points and temperatures, as specified in-figure. Data recorded in flat-plate mode.
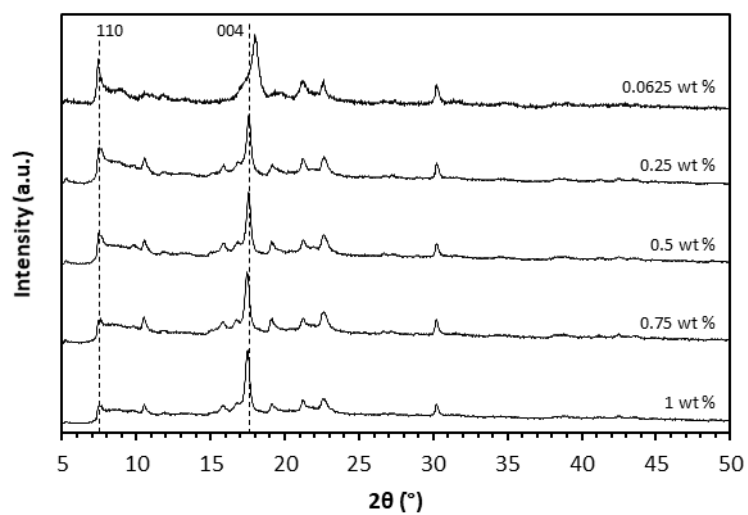
Fig. S6. PXRD patterns of solids produced from varying the reagent concentrations (specified in-figure), using reaction conditions of 120 °C for 1 hr. Data recorded in flat-plate mode.
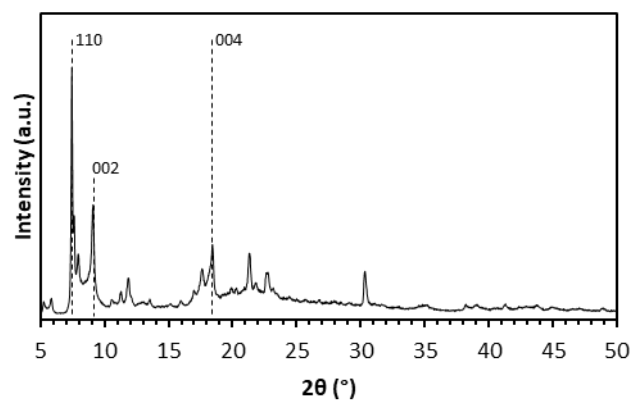
Fig. S7. PXRD pattern of solids produced from "large-scale" batch reaction. Reaction conditions: 1 wt % solids, 120 °C, 3 hrs. N.B. Data recorded in capillary mode, rather than flat plate, so preferred orientation is minimised, leading to differences in relative intensity of peaks compared to other batch syntheses.
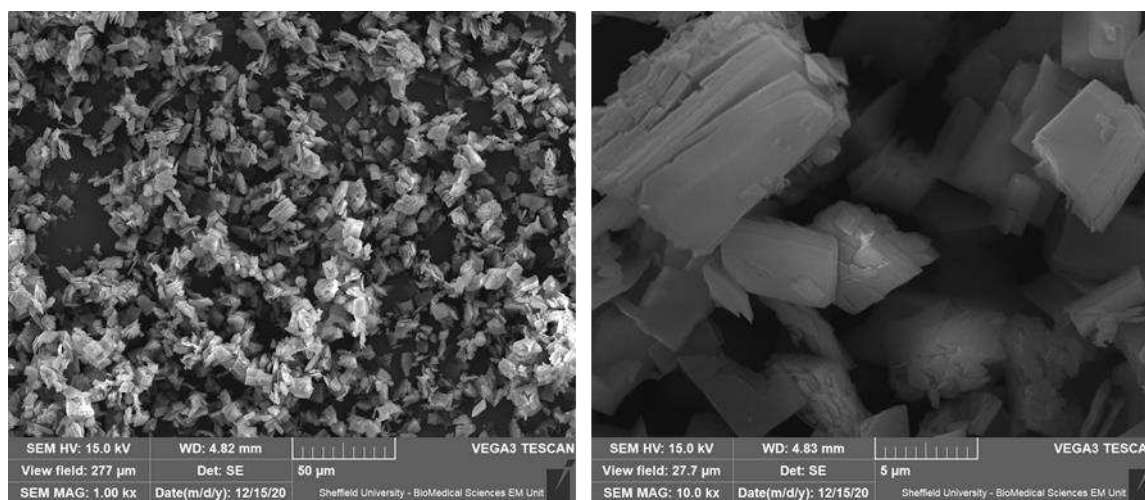
Fig. S8. SEM micrographs of solids formed from the "large-scale" batch reaction.

3. Zn$_2$(ZnTCPP) MOF syntheses using CSTR
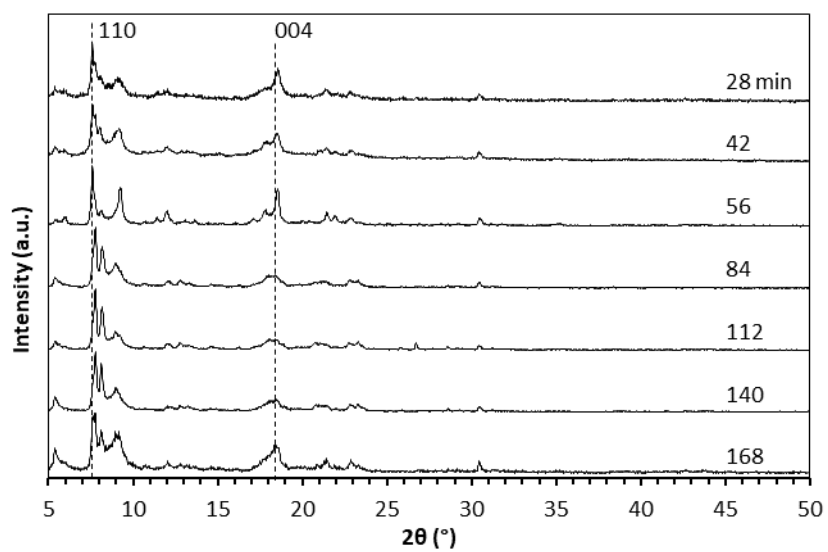
Fig. S9. PXRD patterns of solids produced over time using the initial CSTR set-up at 120°C. Data recorded in flat-plate mode.

4. Zn$_2$(H$_2$TCPP) MON syntheses using batch conditions
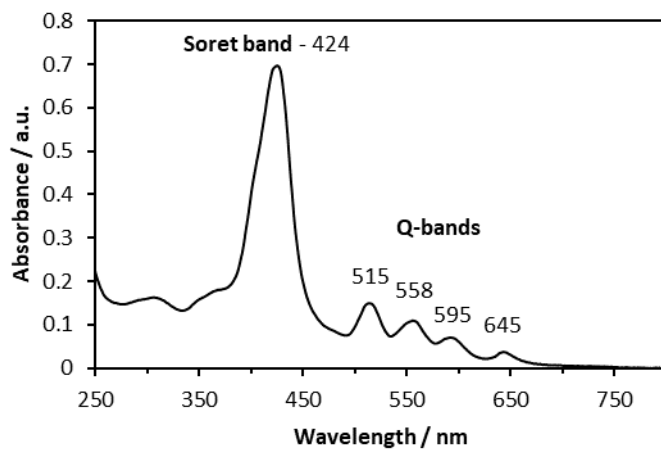
Fig. S10. UV-Vis spectra of MONs produced using triethylamine as an additive at room temperature.
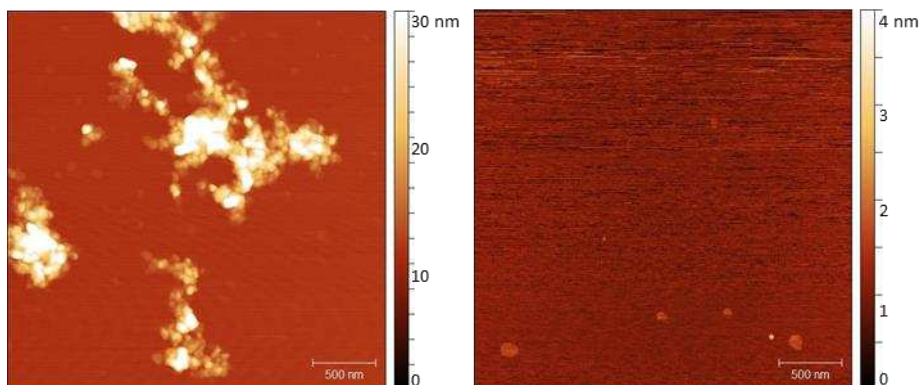
Fig. S11. AFM topographical images of solids formed upon addition of triethylamine to the standard batch synthesis at room temperature, using 3:1 DMF:EtOH ratio.
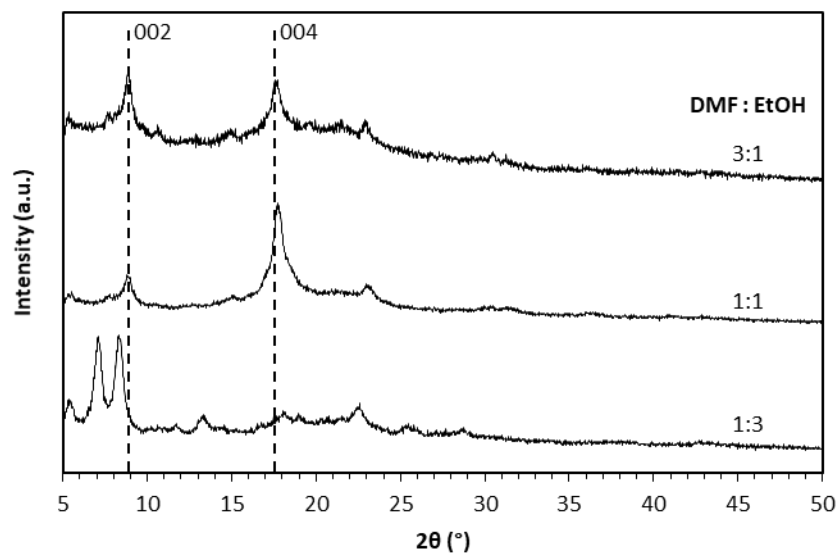
Fig. S12. PXRD patterns of solids formed using different ratios of DMF:EtOH (v:v).
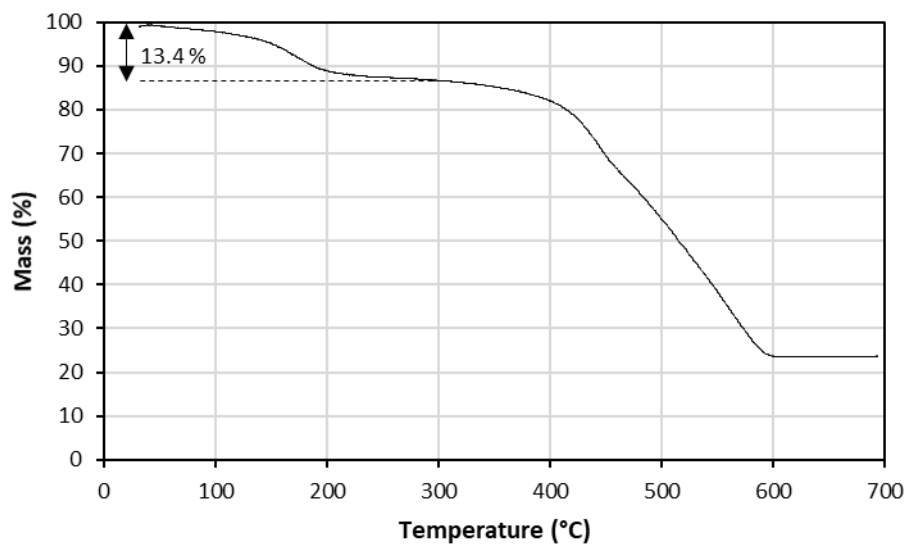
Fig. S13. TGA trace of $Zn_2(H_2TCPP)$ MONs produced from batch synthesis using 1:1 DMF:EtOH (v:v).
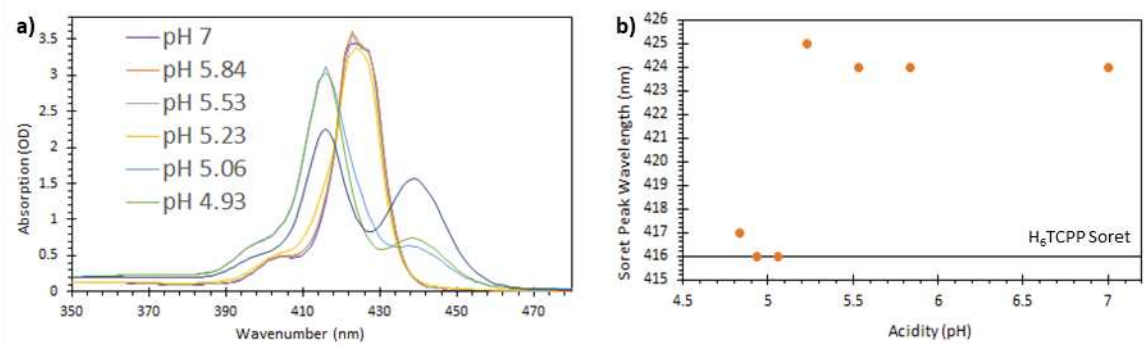
Fig. S14. Phosphoric acid titration of Zn$_2$(H$_2$TCPP) MONs. a) UV-vis spectra at various pH levels, and b) absorbance maxima at different pH levels. The results are interpreted as showing dissolution of the nanosheets below pH 5.3 due to protonation of the porphyrins carboxylate groups.

5. Zn$_2$(H$_2$TCPP) MON syntheses using CSTR
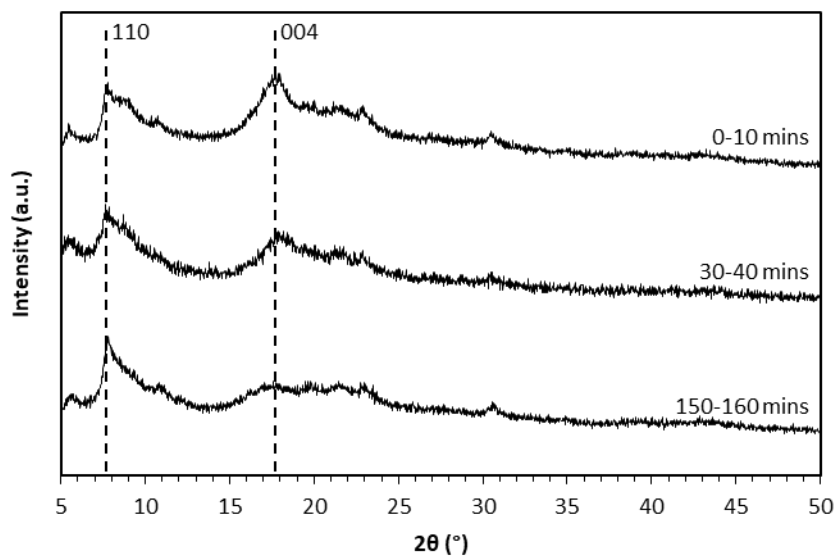
Fig. S15. PXRD patterns of solids collected from fractions indicated in-figure, using CSTR at 25 °C, with triethylamine, using a residence time of 30 mins. Data recorded in flat-plate mode.
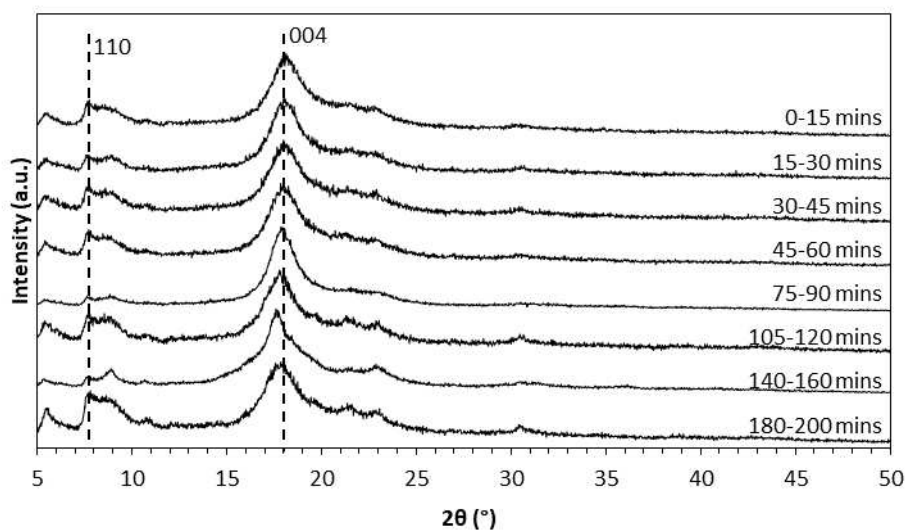
Fig. S16. PXRD patterns of solids produced over time using the CSTR at 25 °C, with triethylamine, using a residence time of 1 hr. Data recorded in flat-plate mode. Solids collected from (top to bottom) fractions 0-15, 15-30, 30-45, 45-60, 75-90, 105-120, 140-160 and 180-200 mins.
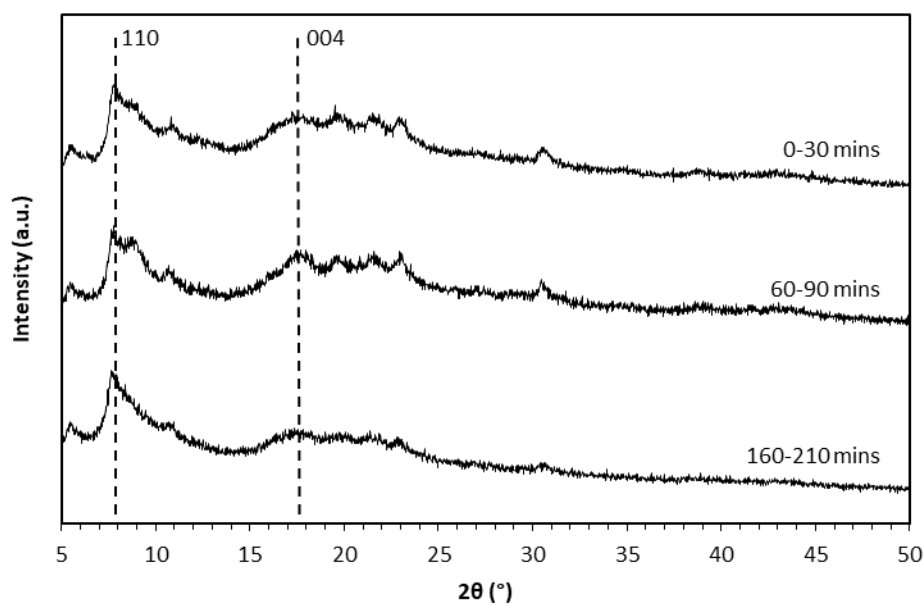
Fig. S17. PXRD patterns of solids collected from fractions indicated in-figure, using CSTR at 25 °C, with triethylamine, using a residence time of 2 hrs. Data recorded in flat-plate mode.
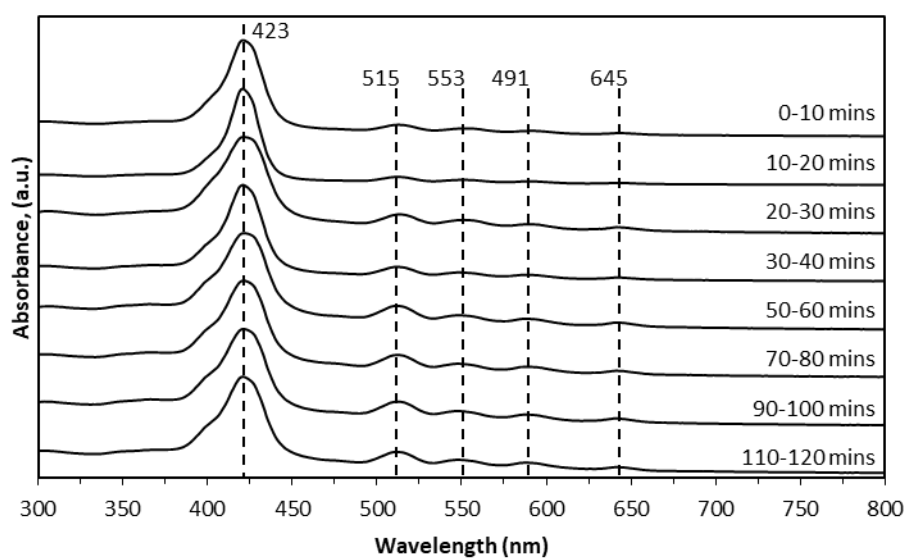
Fig. S18. UV-Vis spectra of dispersed solids collected from fractions indicated in-figure, using the CSTR at 25 °C, with triethylamine, using a residence time of 30 mins.
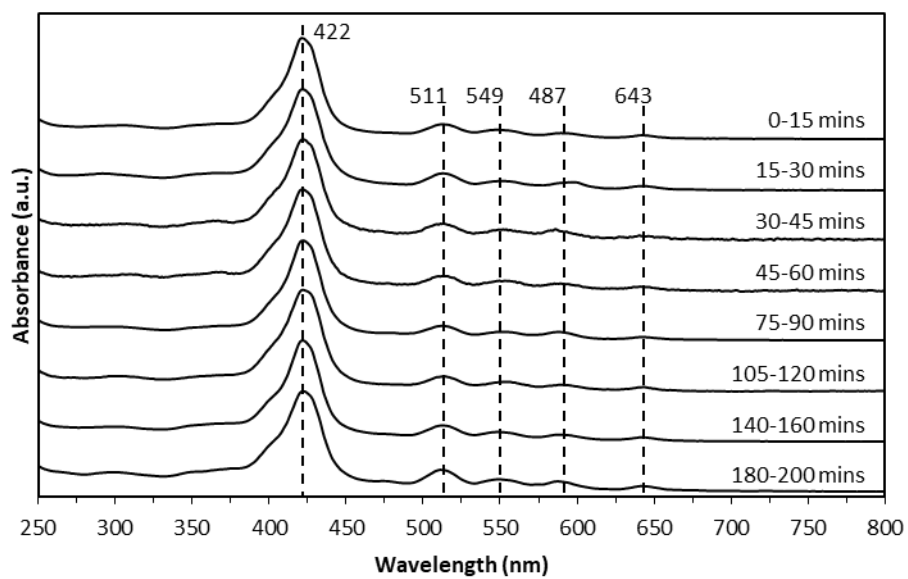
Fig. S19. UV-Vis spectra of dispersed solids collected from fractions indicated in-figure, using the CSTR at 25 °C, with triethylamine, using a residence time of 1 hr.
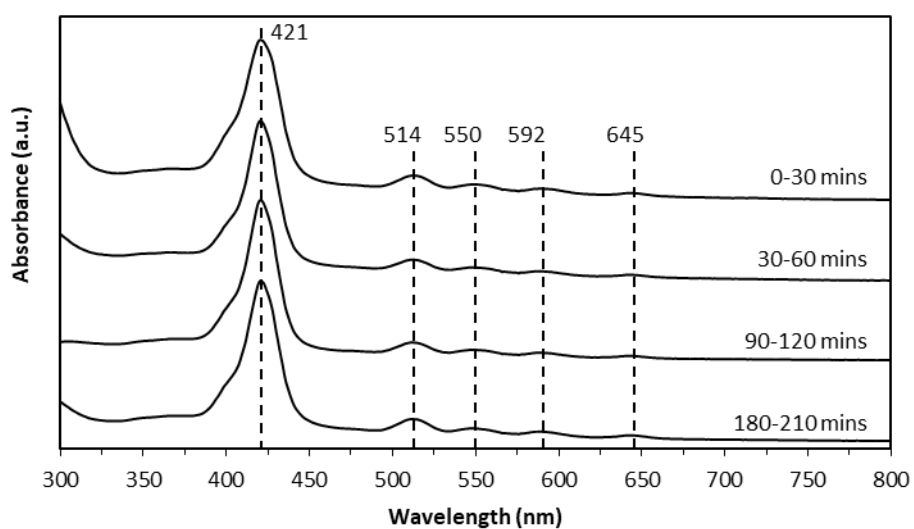
Fig. S20. UV-Vis spectra of dispersed solids collected from fractions indicated in-figure, using the CSTR at 25 °C, with triethylamine, using a residence time of 2 hrs.
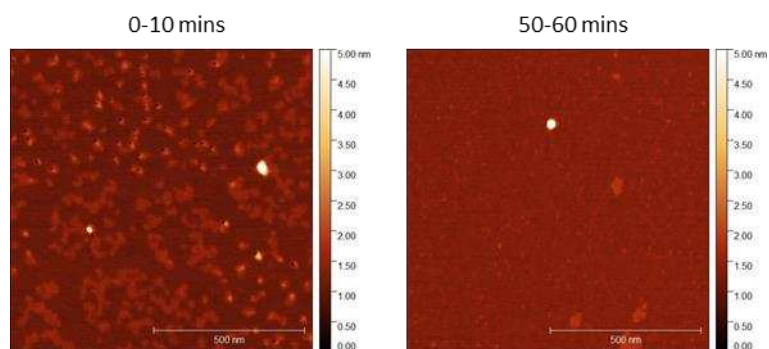
Fig. S21. AFM topographical images of MONs collected in fractions indicated in-figure, using a residence time of 30 mins.
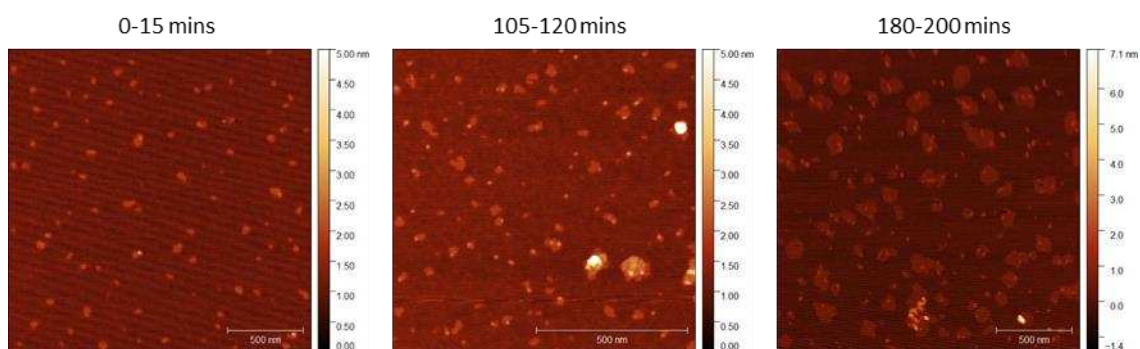
Fig. S22. AFM topographical images of MONs collected in fractions indicated in-figure, using a residence time of 1 hr.
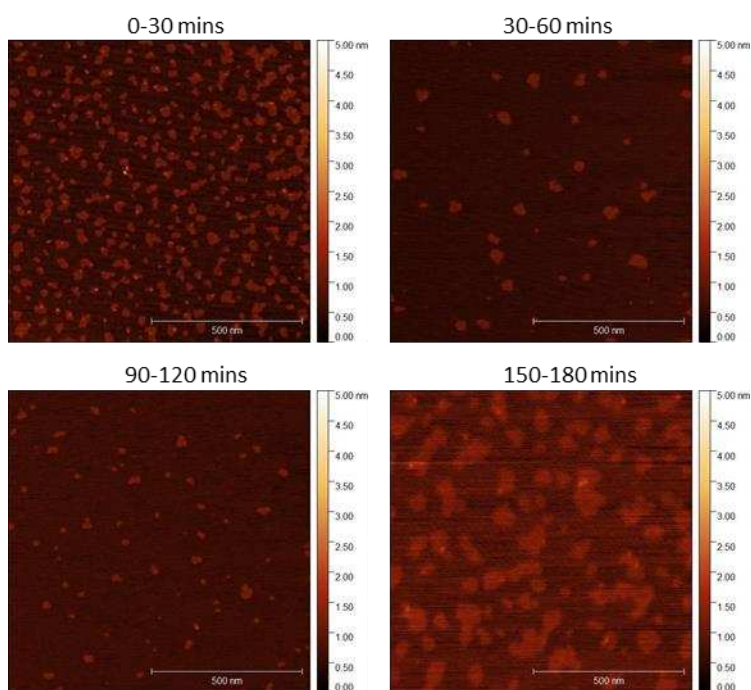
Fig. S23. AFM topographical images of MONs collected in fractions indicated in-figure, using a residence time of 2 hrs.
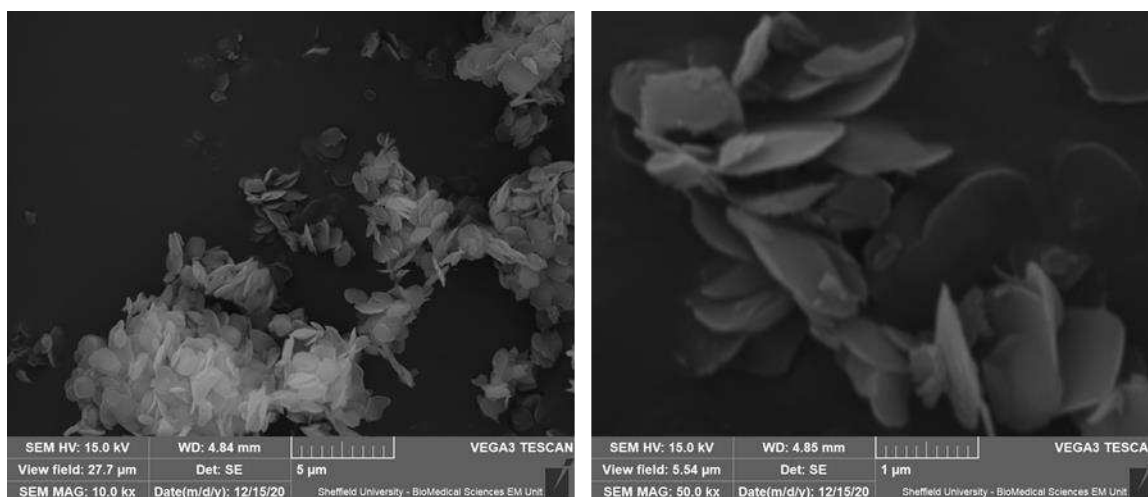
Fig. S24. SEM micrographs of MONs collected from final fraction (180-200 mins), using a residence time of 1 hr.
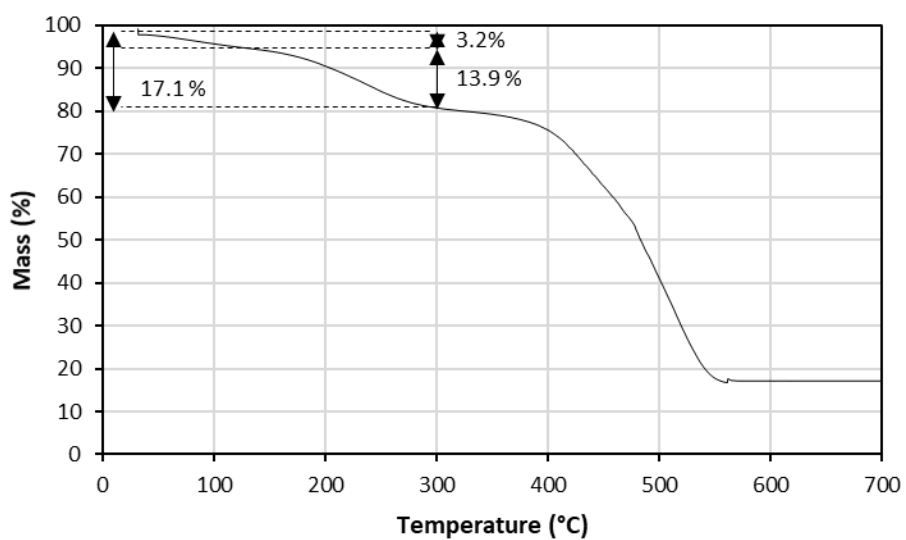
Fig. S25. TGA trace of Zn$_2$(H$_2$TCPP) MONs produced from flow synthesis using *1:1 DMF:EtOH (v:v).*
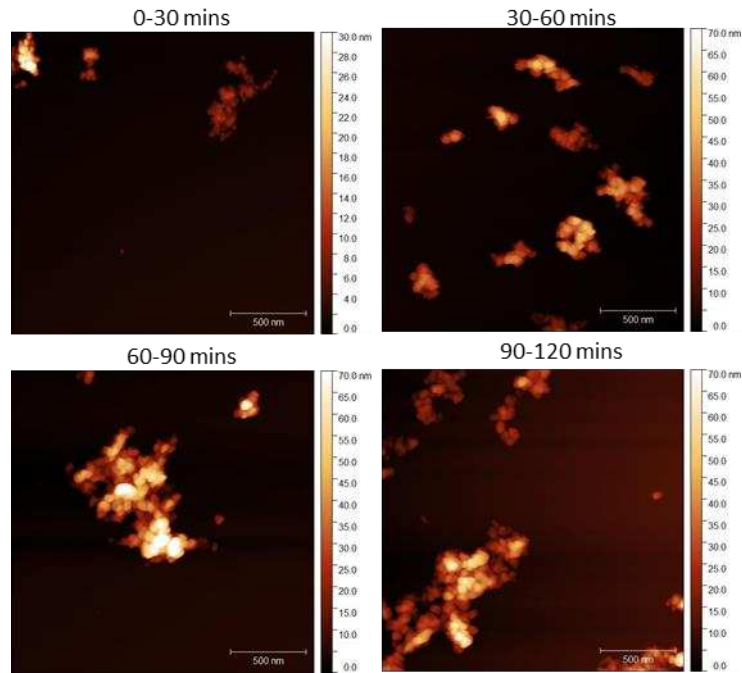
Fig. S26. SEM micrographs of MONs collected from final fraction (180-200 mins), using a residence time of 1 hr.

6. Techno-economic analysis

Table S1. Factors assumed during this work for cost estimation.

| Capital Expenditure (CAPEX)			Operating Expenditure (OPEX)		
Estimation Factor	f_i	Value	Estimation Factor	f_i	Value
Equipment Erection	f_1	0.40	Miscellaneous (Operating)	f_{14}	0.10
Piping	f_2	0.70	Maintenance	f_{15}	0.10
Instrumentation	f_3	0.20	Operating Labour	f_{16}	*Manning Estimates[a]*
Electrical	f_4	0.10	Laboratory Costs	f_{17}	0.30
Buildings, Process	f_5	0.15	Supervision	f_{18}	0.10
Utilities	f_6	0.50	Plant Overheads	f_{19}	0.50
Storages	f_7	0.15	Rates/Local Taxes	f_{20}	0.01
Site Development	f_8	0.05	Insurance	f_{21}	0.01
Ancillary Buildings	f_9	0.15	License Fees/Royalties	f_{22}	0.01
Design and Engineering	f_{10}	0.20	Sales, Overheads, R&D	f_{23}	0.00
Contractor's Fee	f_{11}	0.05			
Contingency	f_{12}	0.10			
Miscellaneous (Capital)	f_{13}	0.20			

[a] Assuming a total of 5 operators (1/shift) salaried at £26,000/ea

Table S2. Method of calculation for capital (CAPEX) and operating (OPEX) expenditure.

Parameter	Method of Calculation
Capital Expenditure (CAPEX)	**CAPEX = FCC + WCC**
Fixed Capital Cost (FCC)	$FCC = PPC \times (1 + f_{10} + f_{11} + f_{12})$
Physical Plant Cost (PPC)	$PPC = PCE \times (1 + f_1 + f_2 + … + f_9)$
Purchase Cost of Equipment (PCE)	$PCE = \sum(C_e)$
Working Capital Cost (WCC)	$WCC = SM + (FCC \times f_{13})$
Stockpiled Materials (SM)	$SM = \sum(C_m)$
Operating Expenditure (OPEX)	**OPEX = DPC + IPC**
Direct Production Cost (DPC)	$DPC = VOC + FOC$
Variable Operating Costs (VOC)	$VOC = M + U + MSC$
Materials (M)	$M = \sum(C_m)$
Utilities (U)	$U = \sum(C_u)$
Miscellaneous Cost (MSC)	$MSC = MC \times f_{14}$
Fixed Operating Cost (FOC)	$FOC = MC + LC + OC$
Maintenance Costs (MC)	$MC = PPC \times f_{15}$
Labour Costs (LC)	$LC = f_{16} \times (1 + f_{17} + f_{18} + f_{19})$
Other Costs (OC)	$OC = FCC \times (f_{20} + f_{21} + f_{22})$
Indirect Production Cost (IPC)	$IPC = DPC \times (f_{23})$

Table S3. Linearised costs for the purchase cost for various equipment (Ce).

Equipment	Costed As	Sizing Parameter, S			Costing Parameters, C_e ($\$_{1987}$)	
		$C = S^a \times 10^b$				
		Parameter	Linearised Range	Unit	a	b
Pump(s)	Centrifugal, conventional	Power	1 to 4	hp	0.257287	2.374268
Reactor	Reactor (Agitated, jacketed)	Volume	30 to 100	us gal	0.547559	2.668311
Cooler(s)	Heat exchanger (Double pipe)	Area	1 to 100	ft^2	0.681589	3.414973
Heater(s)	Heat exchanger (Double pipe)	Area	1 to 100	ft^2	0.681589	3.414973
Mixing Tank(s)	Tank (Agitated, jacketed)	Volume	30 to 100	us gal	0.547559	2.668311
Distillation Tower, Vessel [a]	Column	Diameter	1 to 2	ft	0.43127	2.513627
Distillation Tower, Trays	Column tray	Diameter	1 to 2	ft	[b]	
Distillation Tower, Condenser	Heat exchanger (Double pipe)	Area	1 to 100	ft^2	0.681589	3.414973
Distillation Tower, Reboiler	Heat exchanger (Shell and tube)	Area	100 to 10,000	ft^2	0.689317	2.284123
Filtering Centrifuge	Centrifuge (Solid bowl)	Flowrate	1.5 to 10	t/h	[c]	
Storage Tank(s)	Storage tank (Small)	Capacity	1000 to 20,000	us gal	0.768622	0.694135

[a] Distillation column: Cost parameters show give the cost per height of column ($\$_{1987}$/ft of column height)
[b] Distillation trays: In the examined range there was little variation so a static cost for column trays was assumed (C_e = 300 $\$_{1987}$/tray)
[c] Centrifuge: Original source gave centrifuge costs with linear scaling. Cost were calculated from $C_e = a.S + b$ (where a = 7647, and b = 23,529)

Table S4. Assumed unit prices for materials and utilities.

Materials & Utilities	Unit Price	
	Value	Unit
Chemicals		
Zinc nitrate, $Zn(NO_3)_2$	20.00	$£_{2020}$/kg
Organic ligand, H_2TCPP	3700.00[a]	$£_{2020}$/kg
Dimethyl formamide, DMF	8.00	$£_{2020}$/kg

Ethanol, EtOH	5.00	$£_{2020}$/kg
Triethylamine, TEA	20.00	$£_{2020}$/kg
Utilities		$£_{2020}$/kg
Cooling water	0.001	$£_{2020}$/kg
Steam,	0.02	$£_{2020}$/kg
Electricity	0.14	$£_{2020}$/kWh

[a] See manuscript text about bulk discount methodology.
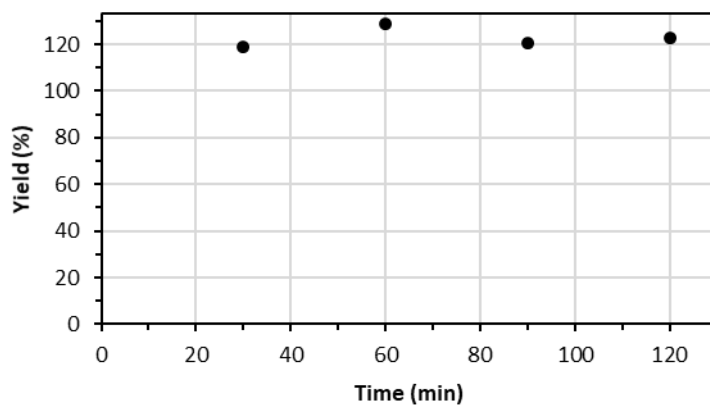
7. Cu$_2$(H$_2$TCPP) MON synthesis using CSTR

Fig. S27. Yield over time, through operation of CSTR to produce Cu$_2$(H$_2$TCPP) MONs. Time points indicate the end of fraction collection.

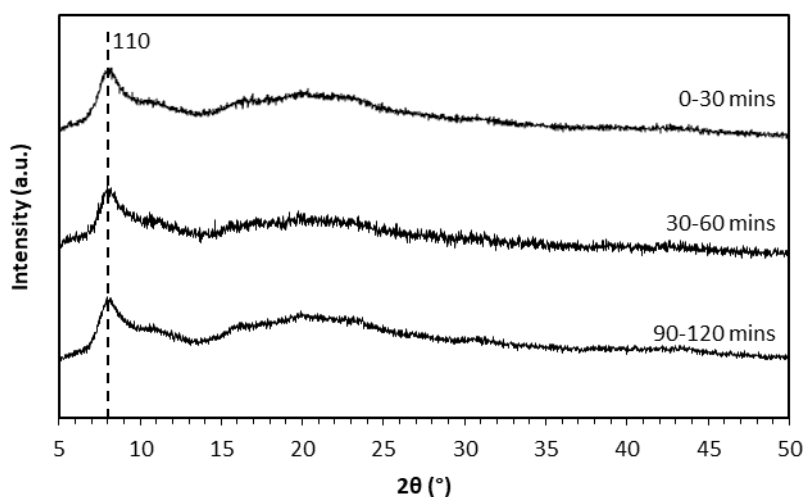*Fig. S28.* PXRD patterns of Cu$_2$(H$_2$TCPP) solids produced over time using the CSTR at 25 °C, with triethylamine, using a residence time of 30 mins. Data recorded in flat-plate mode. Solids collected from fractions indicated in-figure.
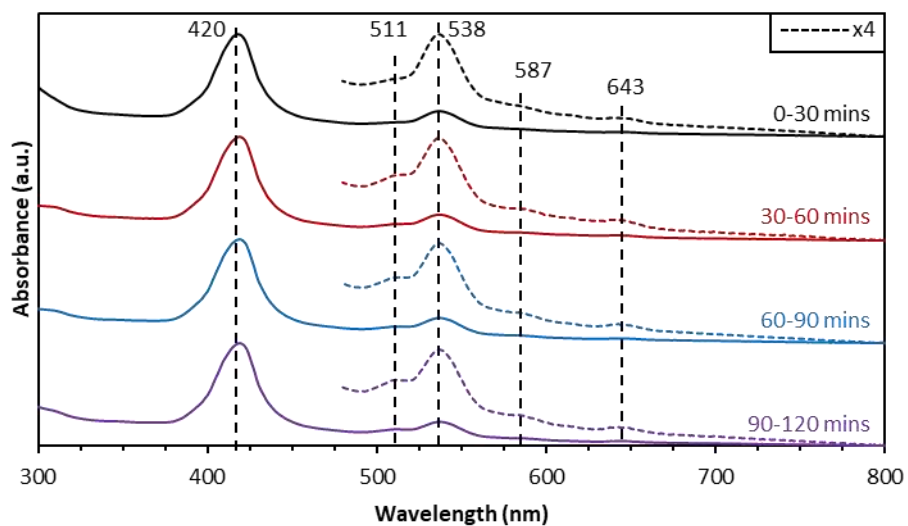
Fig. S29. Offset, normalised UV-Vis spectra of Cu$_2$(H$_2$TCPP) produced from the fractions indicated in-figure. Spectral traces between 480 and 800 nm has also been amplified x4 to aid visualisation (dashed lines).
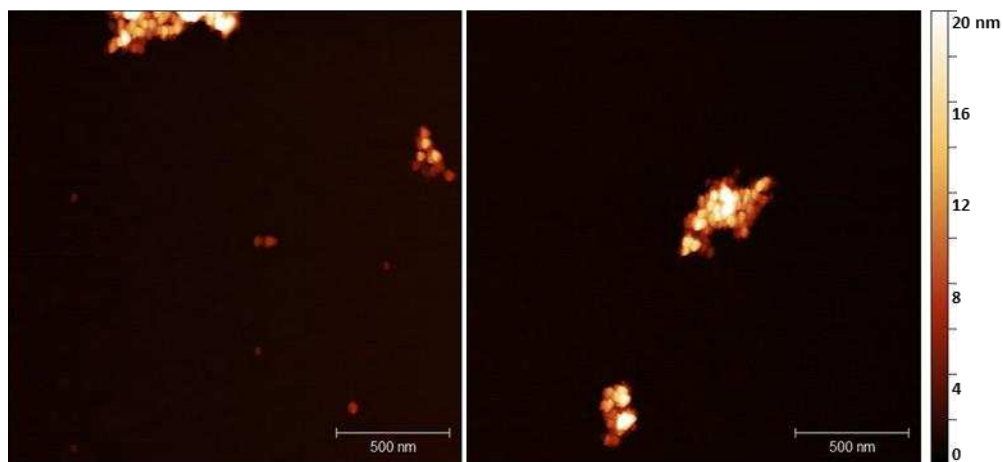

Fig. S30. AFM topographical images of Cu$_2$(H$_2$TCPP) nanosheets, formed from fraction 0-30 (left) and 60-90 (right) mins.

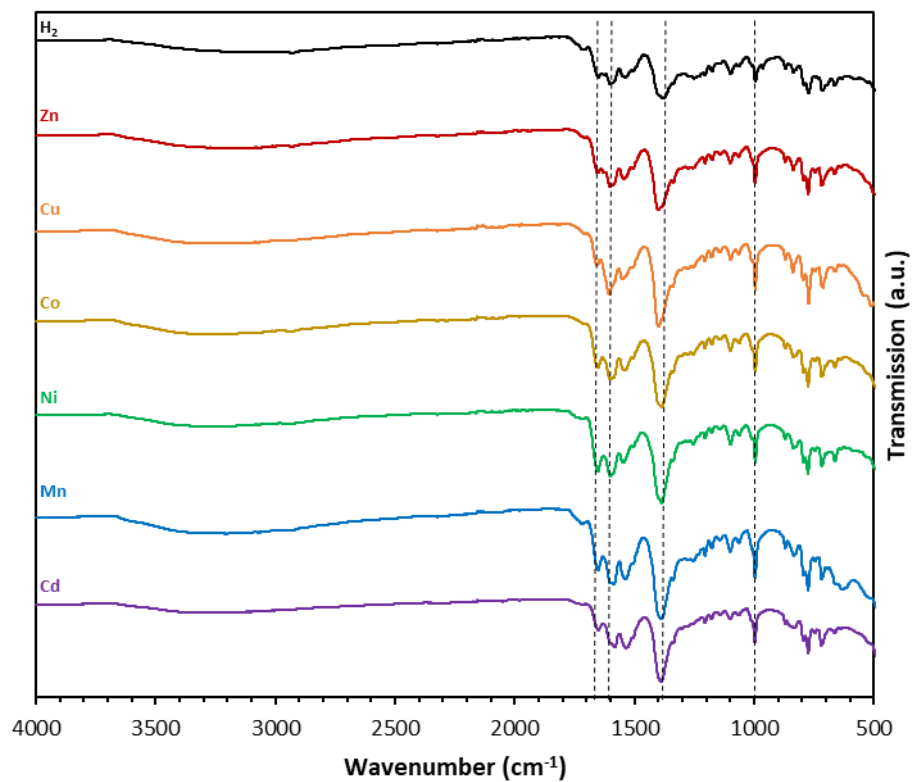## 8. Zn₂(H₂TCPP) MON post-synthetic metalation

Fig. S31. FTIR patterns of solids collected after post-synthetic metalation procedure. Ingoing Zn$_2$(H$_2$TCPP) (top, black), then metalated with Zn, Cu, Co, Ni, Mn and Cd.
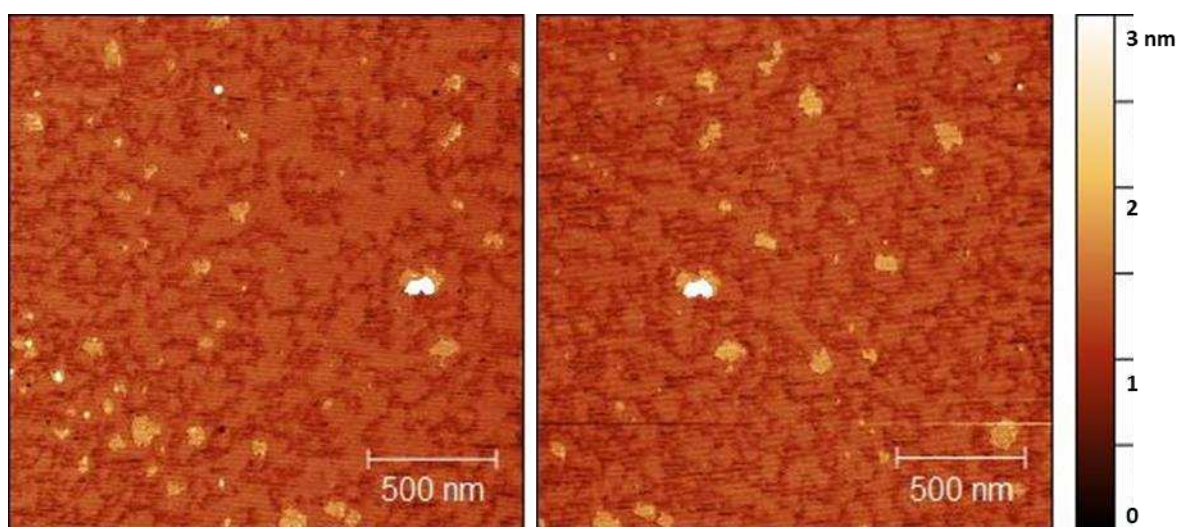

Fig. S32. AFM topographical image of monolayer Zn$_2$(CoTCPP) MONs.

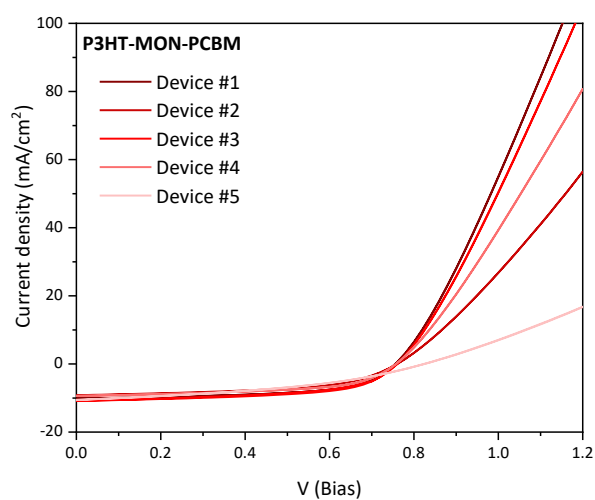# 9. Zn$_2$(H$_2$TCPP) MON application in OPVs

Fig. S33. J-V curves of the evaluated OPV devices with MONs in the photoactive layer.
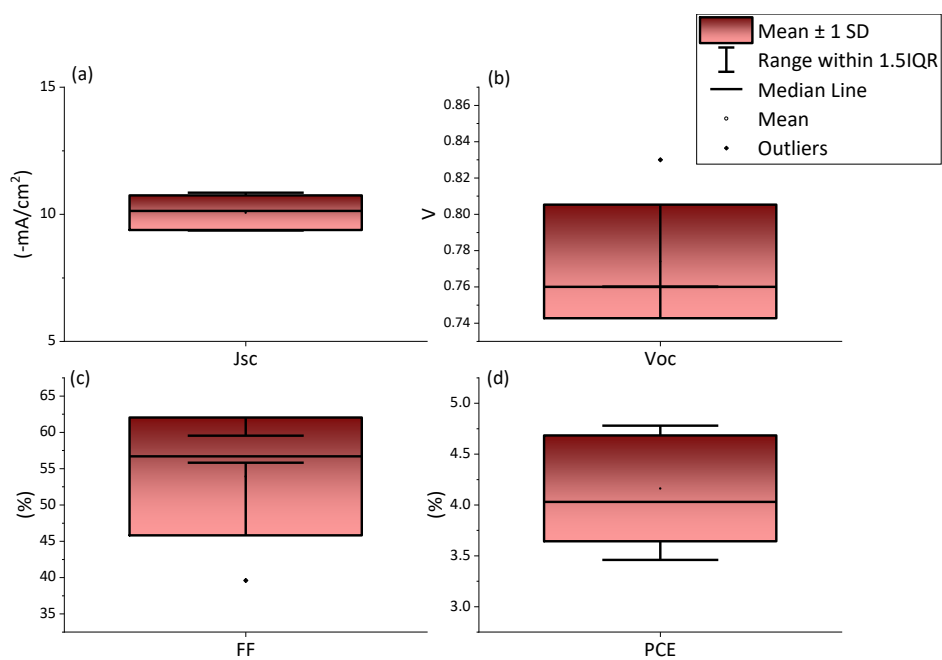

Fig. S34. Statistical analysis of device performance metrics – (a) Jsc, (b) Voc, (c) FF and (d) PCE of the five devices, represented as box plots.